PHYSICAL REVIEW A **81**, 051601(R) (2010)

Bose-Einstein condensation of ^{88}Sr through sympathetic cooling with ^{87}Sr

P. G. Mickelson, Y. N. Martinez de Escobar, M. Yan, B. J. DeSalvo, and T. C. Killian
Rice University, Department of Physics and Astronomy, Houston, Texas 77251, USA
(Received 18 March 2010; published 5 May 2010)

We report Bose-Einstein condensation of ^{88}Sr, which has a small, negative s-wave scattering length ($a_{88} = -2a_0$). We overcome the poor evaporative cooling characteristics of this isotope by sympathetic cooling with ^{87}Sr atoms. ^{87}Sr is effective in this role despite the fact that it is a fermion because of the large ground-state degeneracy arising from a nuclear spin of $I = 9/2$, which reduces the impact of Pauli blocking of collisions. We observe a limited number of atoms in the condensate ($N_{\max} \approx 10^4$) that is consistent with the value of a_{88} and the optical dipole trap parameters.

DOI: 10.1103/PhysRevA.81.051601 PACS number(s): 03.75.Hh, 67.85.Hj

Bose-Einstein condensation of ^{88}Sr has been pursued for over a decade because of the promise of efficient laser cooling to high phase space density using the $(5s^2)\,^1S_0$–$(5s5p)\,^3P_1$ narrow intercombination line [1] and loading of optical dipole traps that operate at the magic wavelength for this transition [2]. Recent interest in ^{88}Sr has focused on long-coherence time interferometers [3], optical frequency standards [4,5], and the existence of low-loss optical Feshbach resonances [6,7]. There has also been great interest generally in quantum degenerate gases of alkaline-earth metal atoms and atoms with similar electronic structures because of potential applications in quantum computing in optical lattices [8–10] and creation of novel quantum fluids [11].

Early attempts to evaporatively cool ^{88}Sr to quantum degeneracy in an optical dipole trap [2,12] were not successful despite initial phase space densities as high as 10^{-1}, presumably because of a small elastic scattering cross section. This was confirmed by measurements of the scattering lengths of all strontium isotopes using photoassociative [13,14] and Fourier-transform [15] spectroscopy of Sr_2 molecular potentials, which found that $a_{88} = -2a_0$, where $a_0 = 5.29 \times 10^{-11}$ m is the Bohr radius. Magnetic Feshbach resonances, which are typically used to overcome poor evaporation properties, do not exist in ^{88}Sr because of its closed-shell ground state and lack of nuclear spin. Here, we report Bose-Einstein condensation (BEC) of ^{88}Sr through sympathetic cooling with ^{87}Sr.

Divalent atoms such as strontium and ytterbium [16,17] often possess a large number of stable isotopes, which enables mass tuning of the s-wave scattering length. For strontium, the stable isotopes and abundances are ^{88}Sr (82.6%),^{87}Sr (7.0%),^{86}Sr (9.9%), and ^{84}Sr (0.6%). In such systems, the likelihood of finding an isotope with a scattering length that enables efficient evaporative cooling is very high, as was recently demonstrated through the condensation of ^{84}Sr ($a_{84} = 123a_0$) [18,19]. For an isotope that has a poor scattering length for evaporative cooling, there are also numerous opportunities to find another isotope that can be used effectively for sympathetic cooling. For ^{88}Sr, the fermionic isotope ^{87}Sr is well suited for this role. It has a large and positive s-wave scattering length of $a_{87} = 96a_0$ [14,15] which leads to efficient thermalization and evaporation as long as the system is not highly polarized. The inter-isotope scattering length is reasonable, $a_{88-87} = 55a_0$ [14,15], so that, in a mixture, collisions with ^{87}Sr will efficiently cool (and evaporate) ^{88}Sr. Dipolar and spin-flip collisional losses are absent because of the closed-shell ground state.

Bosons are normally used to sympathetically cool fermions [20] rather than the other way around, because identical fermions suffer from collisional Pauli blocking, which reduces evaporation efficiency in the quantum degenerate regime [21]. For sympathetic cooling with the bosonic isotopes of strontium, resonant collisions ($a_{86} = 823a_0, a_{88-84} = 1790a_0$) [14,15] should lead to large losses due to three-body collisions [12], which make attaining high densities difficult. We do not observe significant limitations due to Pauli blocking in the experiments reported here, and we suspect this is because ^{87}Sr has a large nuclear spin ($I = 9/2$) and ground-state degeneracy. This suppresses the Fermi temperature and allows ^{88}Sr to be cooled to high phase space density before Pauli blocking of ^{87}Sr collisions becomes important.

Details about our apparatus can be found in Refs. [14,19,25]. Formation of ultracold mixtures of strontium isotopes benefits from the ability to magnetically trap atoms in the metastable $(5s5p)\,^3P_2$ state [12,26–28], which has a 10-min lifetime [29]. One isotope is trapped from a Zeeman slowed beam in a magneto-optical trap (MOT) operating on the $(5s^2)\,^1S_0$–$(5s5p)\,^1P_1$ transition at 461 nm (Fig. 1). This transition is not closed and approximately 1 in 10^5 excitations results in an atom decaying through the $(5s4d)\,^1D_2$ state to the $(5s5p)\,^3P_2$ state, where it can be trapped in the quadrupole magnetic field of the MOT. After accumulating a desired number of atoms, limited by the loading rate and observed $^3P_2$ lifetime of about 25 s, the cooling laser frequency is then changed to cool and accumulate another isotope. In our experiment, we load ^{88}Sr for 3 s and then ^{87}Sr [22] for 30 s. The laser parameters for trapping ^{88}Sr are given in Ref. [26]. For trapping ^{87}Sr [27], the laser is approximately 70 MHz red-detuned from the $^1S_0(F = 9/2)$–$^1P_1(F = 11/2)$ transition (slightly more than 2Γ, where $\Gamma = 30.5$ MHz is the natural linewidth of the transition [30]).

$^3P_2$ atoms are returned to the ground state using 60 ms of 3 W/cm^2 of excitation on the $(5s5p)\,^3P_2$–$(5s4d)\,^3D_2$ transition at 3 μm [25]. The isotope shift ($f_{87} - f_{88} = 110$ MHz) [25] is small compared to the ~500 MHz width of the repumping efficiency curve [31] for ^{88}Sr and the ~3 GHz width of the hyperfine structure in ^{87}Sr [25]. We tune the 3 μm laser 1.6 GHz blue-detuned from the ^{88}Sr resonance,

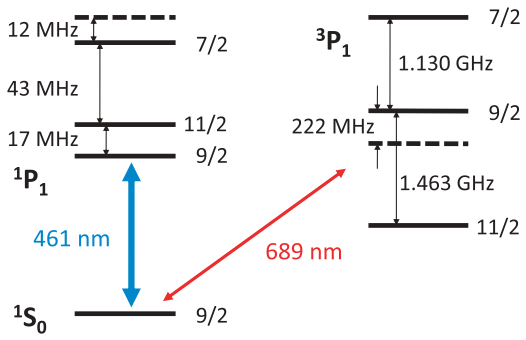

FIG. 1. (Color online) Partial level diagram for ^{88}Sr (- -) and ^{87}Sr (—) showing hyperfine structure and isotope shifts [22–24]. Total quantum number F is indicated for ^{87}Sr levels.

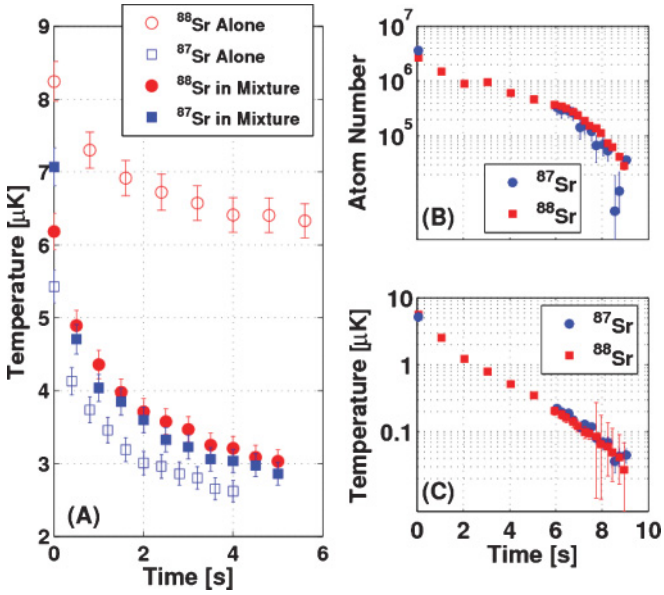

FIG. 2. (Color online) (A) Temperature evolution in an ODT with a trap depth of $U/k_B = 23\ \mu$K for samples of ^{88}Sr and ^{87}Sr alone and for each in a mixture. The number of each isotope present initially is approximately 10^6. (B) Number and (C) temperature for a mixture along a typical forced evaporation trajectory.

which optimizes the ^{87}Sr repumping while reducing the ^{88}Sr number by 80%. This is a reasonable compromise given that the number of ^{87}Sr atoms is the limiting factor in the experiment. The 461 nm MOT is left on at the optimal ^{87}Sr detuning to maximize the number of captured ^{87}Sr atoms, but this is only ∼5 natural linewidths red-detuned of the ^{88}Sr $^1S_0$–$^1P_1$ transition [22,23], so it also serves to aid recapture of this isotope. We typically recapture approximately 1.1×10^7 ^{88}Sr and 3×10^7 ^{87}Sr at temperatures of a few millikelvin.

The 461 nm light is then extinguished and 689 nm light is applied to drive the $(5s^2)\,^1S_0$–$(5s5p)\,^3P_1$ transitions (Fig. 1) and create intercombination-line MOTs for each isotope. The resonance frequencies in each isotope are well-resolved compared to the 7.4 kHz transition linewidth, so the simultaneous MOTs are compatible with each other. The parameters of the $^1S_0$–$^3P_1$ lasers for ^{88}Sr and ^{87}Sr [31] are similar to the conditions in Ref. [1] and Ref. [32], respectively. As many as 70% of the atoms are initially captured in the intercombination-line MOT. (For experiments with one isotope, the intercombination-line lasers for the other isotope are omitted.)

After 400 ms of $^1S_0$-$^3P_1$ laser cooling, an optical dipole trap (ODT) consisting of two crossed beams is overlapped for 100 ms with the intercombination-line MOT with modest power (3.9 W) per beam. The ODT is formed by a single beam derived from a 20 W multimode, 1.06 μm fiber laser that is recycled through the chamber to produce a trap with equipotentials that are nearly oblate spheroids, with the tight axis close to vertical. Each beam has a waist of approximately $w = 90\ \mu$m in the trapping region.

Immediately after extinction of the 689 nm light, the ODT power is ramped in 30 ms to 7.5 W to obtain a trap depth of 25 μK. Typically the atom number, temperature, and peak density at this point for both ^{88}Sr and ^{87}Sr are 3×10^6, 7 μK, and 2.5×10^{13} cm^{-3}. The peak phase space density (PSD) for ^{88}Sr is 10^{-2}.

For diagnostics, we record $^1S_0$–$^1P_1$ resonant absorption images of samples after a time of flight varying from 10 to 40 ms. Because of broadening of the resonance due to hyperfine structure, the ^{87}Sr atoms present would contribute significantly to the absorption when imaging at the ^{88}Sr resonance frequency. To remove ^{87}Sr atoms and obtain clean ^{88}Sr images, light resonant with the $^1S_0(F = 9/2)$–$^3P_1(F = 11/2)$ transition in ^{87}Sr is applied during the first 2 ms of the time of flight. ^{87}Sr atoms are imaged with linearly polarized light resonant with the $^1S_0(F = 9/2)$–$^1P_1(F = 11/2)$ transition, and the contamination due to ^{88}Sr is small and easily accounted for [31].

To investigate the collisional properties of the different isotopes and the mixture, the evolution of number and temperature was recorded in a fixed potential [Fig. 2(A)]. For ^{88}Sr alone, evaporation is inefficient and a typical ratio of the trap depth to the sample temperature is $\eta \approx 4$, as observed previously [12]. ^{87}Sr, however, approaches $\eta \approx 9$. Modeling [33] of the free-evaporation trajectory for ^{87}Sr alone suggests a moderate degree of polarization [31] that will be investigated in future studies. The temperatures of ^{87}Sr and ^{88}Sr atoms in a mixture with peak densities of 8×10^{12} cm^{-3} track each other closely and approach $\eta \approx 8$, indicating that ^{87}Sr provides efficient sympathetic cooling of ^{88}Sr.

Figure 2 shows the number (B) and temperature (C) for a typical forced evaporation trajectory with a mixture. We decrease the laser power according to $P = P_0/(1 + t/\tau)^\beta + P_{\text{offset}}$, with time denoted by t, $\beta = 1.4$, and $\tau = 1.5$ s. This trajectory without P_{offset} was designed [34] to yield efficient evaporation when gravity can be neglected. Gravity is a significant effect in this trap for Sr, and to avoid decreasing the potential depth too quickly at the end of the evaporation, we set $P_{\text{offset}} = 0.7$ W, which corresponds to the power at which gravity causes the trap depth to be close to zero. The lifetime of atoms in the ODT is 30 s. This allows efficient evaporation and an increase of PSD by a factor of 100 for a loss of one order of magnitude in the number of atoms. The ^{87}Sr and ^{88}Sr remain in equilibrium with each other during

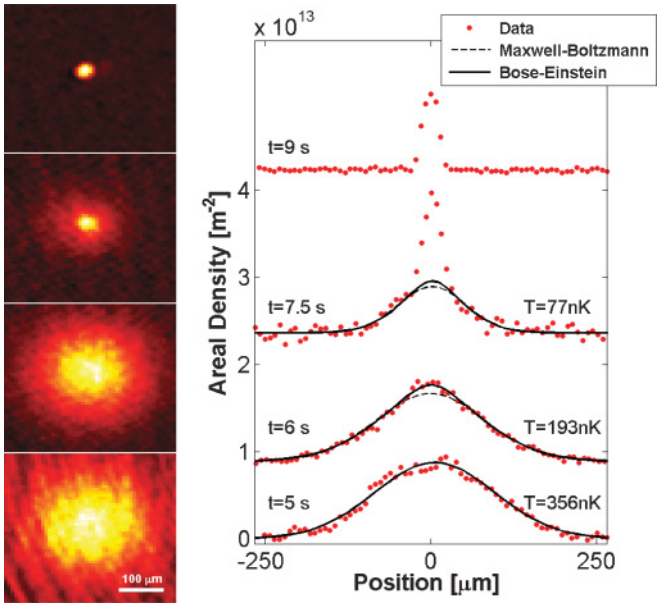

FIG. 3. (Color online) Appearance of Bose-Einstein condensation in absorption images (left) and areal density profiles (right). Data correspond to 16 ms (bottom) or 22 ms (top three) of free expansion after indicated evaporation times (t). Images on the left have the same time stamp as on the right. The areal density profiles are from a vertical cut through the center of the atom cloud, and temperatures are extracted from two-dimensional Bose-Einstein distribution fits to the thermal pedestal. At 7.5 s, a bimodal distribution is evident, indicative of Bose-Einstein condensation. A pure condensate is shown at 9 s of evaporation. The Maxwell-Boltzmann distribution does not accurately describe low-velocity atoms near degeneracy, and the Bose-Einstein distribution does not describe the condensate contribution. So in these respective regimes, a central region slightly larger than the condensate radius is excluded from fitting. For bimodal data, fugacity is constrained to 1.

the evaporation. ^{87}Sr atoms are lost at a slightly faster rate, as expected because essentially every collision involves an ^{87}Sr atom.

Figure 3 shows false color two-dimensional renderings of (left) and one-dimensional slices through (right) the time-of-flight absorption images recorded after 16 or 22 ms of expansion for various points along the evaporation trajectory. At 5 s of evaporation, the distribution is fit well by a Maxwell-Boltzmann distribution, but at 6 s, a Boltzmann distribution fit to the high-velocity wings clearly underestimates the number of atoms at low velocity. A fit using the Bose-Einstein distribution [35], however, matches the distribution well. The fugacity obtained from this fit is 1.0, indicating this is close to the critical temperature for condensation. With further evaporation (7.5 s), a narrow peak emerges at low velocity. This bimodal distribution is a clear signature of the presence of a Bose-Einstein condensate. A pure condensate is observed near the end of the evaporation trajectory (9 s).

At the transition temperature, 2×10^5 ^{87}Sr atoms remain at a temperature of 0.2 μK. This corresponds to $T/T_F = 0.9$ for an unpolarized sample, which is nondegenerate and above the point at which Pauli blocking significantly impedes evaporation efficiency [21].

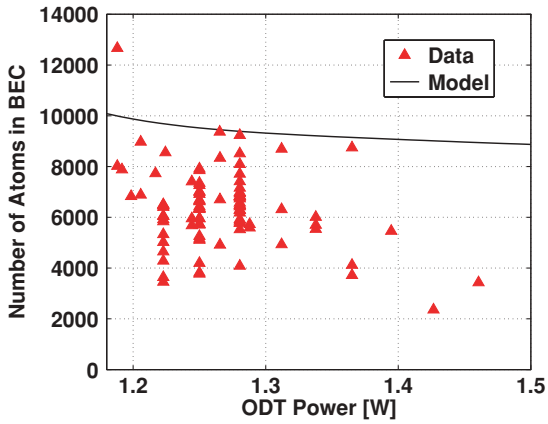

FIG. 4. (Color online) Comparison of observed condensate number and maximum condensate number predicted by a model of the trapping potential along the evaporation trajectory.

^{88}Sr has a negative scattering length, so one expects a collapse of the condensate when the system approaches a critical number of condensed atoms given by [36]

$$N_{\rm cr} = 0.575 \frac{a_{\rm ho}}{|a_{88}|}. \quad (1)$$

Here $a_{\rm ho} = [\hbar/(m\overline{\omega})]^{1/2}$ is the harmonic oscillator length, where m is the atom mass, $\hbar$ is the reduced Planck constant, and $\overline{\omega} = (\omega_x\omega_y\omega_z)^{1/3}$ is the geometric average of the oscillator frequencies. One should also see large fluctuations in the number of condensed atoms during the evaporation due to repeated collapses and refilling of the condensate. To investigate this, we recorded the condensate number for various points in the evaporation trajectory over many experimental runs. For absorption images with a condensate and thermal pedestal, we fit the wings of the thermal cloud, which are beyond the condensate radii of about 23 μm, to a Bose distribution with fugacity set to 1. The residuals of the fit represent the condensate atoms which are fit with the standard Thomas-Fermi functional form [19,37] to determine their number.

Figure 4 shows the observed condensate number along the evaporation trajectory from 7 to 10 s, as well as the maximum values of $N_{\rm cr}$ predicted by Eq. (1) for a waist of $w = 100$ μm and $a_{88} = -1.6a_0$, which are within the uncertainty ranges for these parameters. Uncertainties in knowledge of the trap become larger at low ODT power because of the increasingly important role of gravity, which weakens the trap. Significant variation in condensate number is seen. A model of the atom kinetics would be required to make a quantitative statement about the agreement between the observed and the expected number distributions.

We have described Bose-Einstein condensation of ^{88}Sr through sympathetic cooling with ^{87}Sr. The observed maximum number of condensed atoms is consistent with the small, negative value of a_{88}. Because of the weak interactions, it should be possible to change the sign of the scattering length with an optical Feshbach resonance [6,7] while keeping induced inelastic losses low. This suggests many possible

future experiments, such as the creation of matter-wave solitons in two dimensions [38] and quantum fluids with random nonlinear interactions [39].

This research was supported by the Welch Foundation (C-1579), the National Science Foundation (PHY-0855642), and the Keck Foundation.

[1] H. Katori, T. Ido, Y. Isoya, and M. Kuwata-Gonokami, Phys. Rev. Lett. **82**, 1116 (1999).
[2] T. Ido, Y. Isoya, and H. Katori, Phys. Rev. A **61**, 061403(R) (2000).
[3] G. Ferrari, N. Poli, F. Sorrentino, and G. M. Tino, Phys. Rev. Lett. **97**, 060402 (2006).
[4] C. Lisdat, J. S. R. V. Winfred, T. Middelmann, F. Riehle, and U. Sterr, Phys. Rev. Lett. **103**, 090801 (2009).
[5] T. Akatsuka, M. Takamoto, and H. Katori, Phys. Rev. A **81**, 023402 (2010).
[6] R. Ciurylo, E. Tiesinga, and P. S. Julienne, Phys. Rev. A **71**, 030701(R) (2005).
[7] K. Enomoto, K. Kasa, M. Kitagawa, and Y. Takahashi, Phys. Rev. Lett. **101**, 203201 (2008).
[8] A. J. Daley, M. M. Boyd, J. Ye, and P. Zoller, Phys. Rev. Lett. **101**, 170504 (2008).
[9] A. V. Gorshkov *et al.*, Phys. Rev. Lett. **102**, 110503 (2009).
[10] I. Reichenbach, P. S. Julienne, and I. H. Deutsch, Phys. Rev. A **80**, 020701(R) (2009).
[11] M. Hermele, V. Gurarie, and A. M. Rey, Phys. Rev. Lett. **103**, 135301 (2009).
[12] G. Ferrari, R. E. Drullinger, N. Poli, F. Sorrentino, and G. M. Tino, Phys. Rev. A **73**, 023408 (2006).
[13] P. G. Mickelson *et al.*, Phys. Rev. Lett. **95**, 223002 (2005).
[14] Y. N. Martinez de Escobar *et al.*, Phys. Rev. A **78**, 062708 (2008).
[15] A. Stein, H. Knöckel, and E. Tiemann, Eur. Phys. J. D **57**, 171 (2010).
[16] T. Fukuhara, S. Sugawa, Y. Takasu, and Y. Takahashi, Phys. Rev. A **79**, 021601(R) (2009).
[17] T. Fukuhara *et al.*, J. Low Temp. Phys. **148**, 441 (2007).
[18] S. Stellmer, M. K. Tey, B. Huang, R. Grimm, and F. Schreck, Phys. Rev. Lett. **103**, 200401 (2009).
[19] Y. N. Martinez de Escobar *et al.*, Phys. Rev. Lett. **103**, 200402 (2009).
[20] A. G. Truscott *et al.*, Science **291**, 2570 (2001).
[21] B. DeMarco and D. S. Jin, Science **285**, 1703 (1999).
[22] X. Xu *et al.*, Phys. Rev. Lett. **90**, 193002 (2003).
[23] K. Ko *et al.*, J. Opt. Soc. Am. B **23**, 2465 (2006).
[24] I. Courtillot *et al.*, Eur. Phys. J. D **33**, 161 (2005).
[25] P. G. Mickelson *et al.*, J. Phys. B **42**, 235001 (2009).
[26] S. B. Nagel *et al.*, Phys. Rev. A **67**, 011401(R) (2003).
[27] X. Xu *et al.*, J. Opt. Soc. B **20**, 968 (2003).
[28] N. Poli *et al.*, Phys. Rev. A **71**, 061403(R) (2005).
[29] M. Yasuda and H. Katori, Phys. Rev. Lett. **92**, 153004 (2004).
[30] S. B. Nagel *et al.*, Phys. Rev. Lett. **94**, 083004 (2005).
[31] P. G. Mickelson, Ph.D. thesis, Rice University, 2010.
[32] T. Mukaiyama, H. Katori, T. Ido, Y. Li, and M. Kuwata-Gonokami, Phys. Rev. Lett. **90**, 113002 (2003).
[33] M. Yan *et al.*, e-print arXiv:0905.2223.
[34] K. M. O'Hara, M. E. Gehm, S. R. Granade, and J. E. Thomas, Phys. Rev. A **64**, 051403(R) (2001).
[35] W. Ketterle, D. S. Durfee, and D. M. Stamper-Kurn, in *Proceedings of the International School of Physics-Enrico Fermi*, edited by M. I. *et al.* (IOS Press, Amsterdam, 1999), p. 67.
[36] P. A. Ruprecht, M. J. Holland, K. Burnett and M. Edwards, Phys. Rev. A **51**, 4704 (1995).
[37] F. Dalfovo *et al.*, Rev. Mod. Phys. **71**, 463 (1999).
[38] H. Saito and M. Ueda, Phys. Rev. Lett. **90**, 040403 (2003).
[39] M. P. A. Fisher, P. B. Weichman, G. Grinstein, and D. S. Fisher, Phys. Rev. B **40**, 546 (1989).